JOURNAL OF combinatorial CHEMISTRY

Article

Colorimetric Diffusion-Reflection Imaging High-Throughput Analysis of Organic or Inorganic Compounds

Jiang P. Yi, Li Huang, Zheng W. Jiang, Wen S. Li, and Xiao P. Zhou

J. Comb. Chem., **2006**, 8 (6), 881-889• DOI: 10.1021/cc0600730 • Publication Date (Web): 19 October 2006

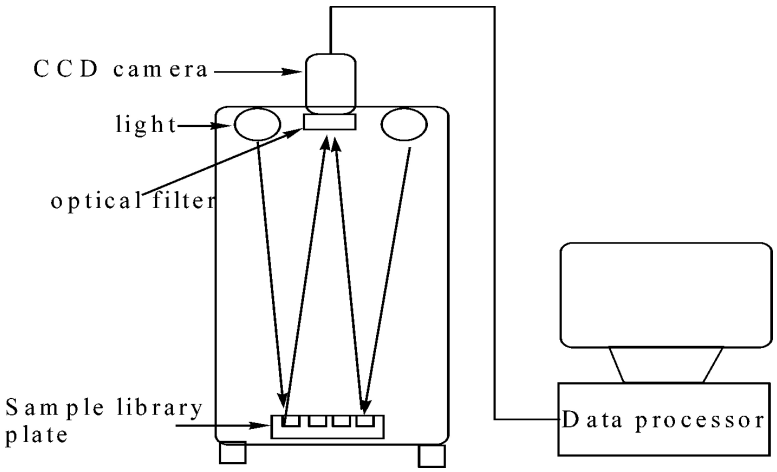

More About This Article

Additional resources and features associated with this article are available within the HTML version:

- Supporting Information
- Links to the 1 articles that cite this article, as of the time of this article download
- Access to high resolution figures
- Links to articles and content related to this article
- Copyright permission to reproduce figures and/or text from this article

View the Full Text HTML

Journal of Combinatorial Chemistry is published by the American Chemical Society.
1155 Sixteenth Street N.W., Washington, DC 20036

Colorimetric Diffusion-Reflection Imaging High-Throughput Analysis of Organic or Inorganic Compounds

Jiang P. Yi, Li Huang, Zheng W. Jiang, Wen S. Li, and Xiao P. Zhou*

Department of Chemical Engineering, Hunan University, Changsha 410082, China

Received June 4, 2006

A colorimetric diffusion-reflection imaging (CDRI) high-throughput analytical technology was developed for library analysis. In the investigation, quartz sands were employed as light diffusion−reflection media. Inorganic and organic compounds with characteristic absorption bands in visible light could be quantified by this method. In the current investigation, compounds such as $CrCl_3$, $KMnO_4$, methylene blue, and acrolein were employed as substrates, and the UV spectrometer and traditional GC (with thermal conductivity detector) were employed to check the reliability of our CDRI technology. The current technology is capable of analyzing more then 100 samples simultaneously. Relative errors below 10% were achieved.

1. Introduction

Recently, IR thermography,[1−3] photofluorescence imaging,[4] laser-induced resonance-enhanced multiphoton ionization,[5] HPLC screening technology,[6] microprobe sampling mass spectrometry,[7−8] and fluorescence indicators[9−10] have been developed for high-throughput catalyst screening. IR thermography can measure the temperature variation over libraries. Hence, the Moates,[1] Taylor,[2] and Wilson[3] groups employed the technology to scan catalysts for exothermic reactions. IR thermography is a universally thermal-sensitive technology, which responds to any exothermal and endothermic reactions. Therefore, it was employed in catalyst screening, such as the combustion reactions of CO and H_2 or the NO_x-involved combustion reactions. Previously, we have developed a photofluorescence imaging technology for photodegradation catalyst screening.[4] This technology could be widely applicable in the analysis of compounds, which emit fluorescent light under the irradiation of UV light or electron beam or in the analysis of compounds that could be converted to fluorescent compounds through chemical reactions. However, it is not valid for the analysis of chemicals that do not emit fluorescent light under the irradiation of UV light or electron beam. Suzuki and coworkers developed a pH-imaging high-throughput technology for photocatalyst screening. The analysis technology is valid for reactions that have acidity variation.[11] The UV laser-induced resonance-enhanced multiphotoionization technology developed by Senkan et al.[5] is a high-throughput technology, which is capable of selectively detecting compounds with different ionization energies. In catalyst screening for hydrogen preparation, McFarland et al. developed a high-throughput hydrogen detection technology, which is capable of screening large catalyst libraries.[6] Microprobe sampling mass spectroscopy (MSMS) is a widely applicable technology for high-throughput analysis.[7−8] However, the manufacture of the instrument is too costly for universal applications, especially for researchers at universities. Also, MSMS is actually a robotic serial-detection technology. Currently, although UV−vis high-throughput spectroscopy meters or plate readers are available, such as that made by Molecular Devices Corp., most of them (Supporting Information, part A) are robot-automated serial-analysis machines. They are actually modified from regular UV−vis spectroscopy meters with cells driven by step motors. In this case, the instrument measures samples one-by-one, and the machine includes moving parts and the spectroscopy meter itself. Therefore, the instrument is expensive and complicated to manufacture. Schüth et al.[12] developed an imaging technology in catalyst screening by imaging the color spots generated on substrate (filter paper preloaded with indicator). Because the direct calculation based on the spots on substrates might result in large analysis errors, one can either make the judgment by eye semiquantitatively or cut off the spots, extract the color compound by solvent, and analyze them with a regular UV−vis spectrometer. The throughput is limited. The other drawback of the method is that the amount of organic indicator loaded on substrate is very limited. Therefore, the concentration region that the instrument can measure is very narrow. It is desirable to have a relatively cheap and widely applicable high-throughput technology for library sample analysis.

To obtain a cheap and relatively widely applicable analysis tool, we recently developed a new high-throughput analysis technology based on the colorimetric diffusion−reflection imaging concept. The working principle is that light from the sources irradiates the wells that contain substrate solutions and quartz sands on the testing plate. The incidence light reflects on the surfaces of quartz sands and diffuses into the solution and quartz crystals and then goes through an optical filter to reach the CCD camera. In the diffusion−reflection process, part of the light is absorbed by the substrate solution (the absorption of quartz is relatively small compared with that of the substrate compound in visible light). This instrument is designed to measure the absorption intensity of compounds. The optical filter should be chosen according to the UV spectrum of substrate compound (the passing band

* To whom correspondence should be addressed. Phone: 8607318821017. Fax: 8607318821017. E-mail: hgx2002@hnu.cn.

10.1021/cc0600730 CCC: $33.50
Published on Web 10/19/2006

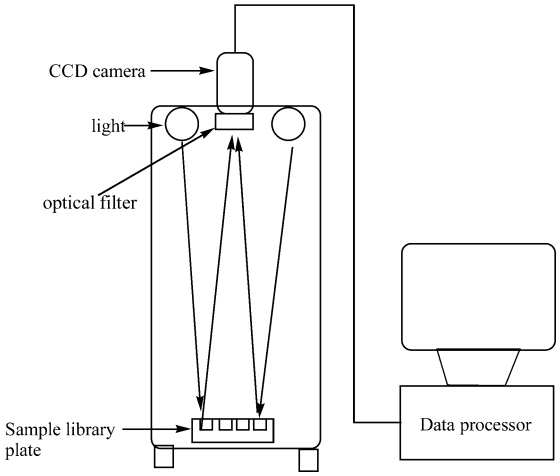

Figure 1. Colorimetric diffusion-reflection imaging system.

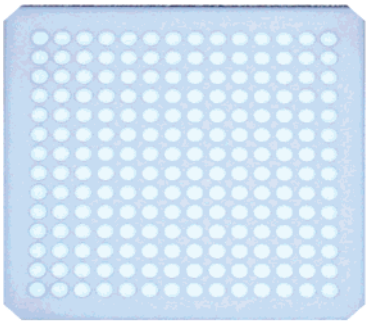

Figure 2. Sample library plate (size 13 × 13 cm). The well diameter and depth are 8.0 and 6.0 mm, respectively.

should match the characteristic absorption band of the substrate). Therefore, before we quantify a compound in library elements by CDRI method, we need to record a UV spectrum of the compound on a regular UV spectrometer. The CCD camera detector is employed to record the intensity of the light from the testing plate. The absorption intensities of substrate solutions can be calculated by subtraction of the intensities of the substrate solutions from the intensities of the blank library (library containing solvent and quartz sands only). The concentrations of the substrate solutions can be calculated from the absorption value; a detailed description of the data recording and processing can be found in the Experimental Section.

2. Experimental Section

2.1. Construction of the Instrument. The instrument was constructed from a 0.56 × 0.6 × 2.0 m box, light sources, CCD camera (SAMSUNG SCC-U1, installed on the ceiling), optical filter, sample library plate (with 14 × 14 or 12 × 12 wells, as shown in Figure 2), and a computer as shown in Figure 1. Two 8 W white mercury fluorescent lights were installed on the ceiling of the box as the light sources. The sample library plate is a 13 × 13 cm polytetrafluoroethylene plate with 14 × 14 or 12 × 12 wells on it. The well diameter and depth are 8.0 and 6.0 mm, respectively. The data collecting and reducing software was designed in our laboratory.

2.2. Analysis of Sample Libraries. In the analysis of sample libraries, we need to record the data of the blank solvent. The blank solvent library was prepared by filling the wells of the sample library plate with quartz sands of particle sizes between 40 and 60 mesh. The extra sand was scratchedaway on the surface of the plate, and it was flattened. To the quartz sand loaded sample plate, an equal amount of solvent (in this work, 65 μL of water) was transferred to the wells to make the blank solvent library, and then the sample library was placed under the CCD camera. (An optical filter matching the characteristic absorption band of substrate should be chosen. Here, an optical filter with a passing band at 600 ± 30 nm (transparency of 70% at 600 nm) was chosen.) A picture, as shown in Figure 3A, was taken. An in-house-designed image integration and data reduction (IIDR) program was employed to integrate the intensity of the light over the individual wells of the plate and to reduce the data. The light intensity data of blank solvent library are listed in Table 1.

After the blank solvent data of the library was collected, we conducted the analysis of the substrate library. In the analysis, a series of standard solution samples with different concentrations of substrate were prepared. The solutions in this example are $CrCl_3$ solutions. The concentrations of the standard samples are 0.0010, 0.010, 0.050, 0.10, 0.15, 0.18, 0.20, 0.30, 0.40, 0.50, 0.60, and 0.80 M, respectively. The concentrations of the testing samples are 0.15 and 0.30 M. The characteristic absorption band of Cr^{3+} is at 595 nm. Hence, an optical filter with a passing band at 600 ± 30 nm

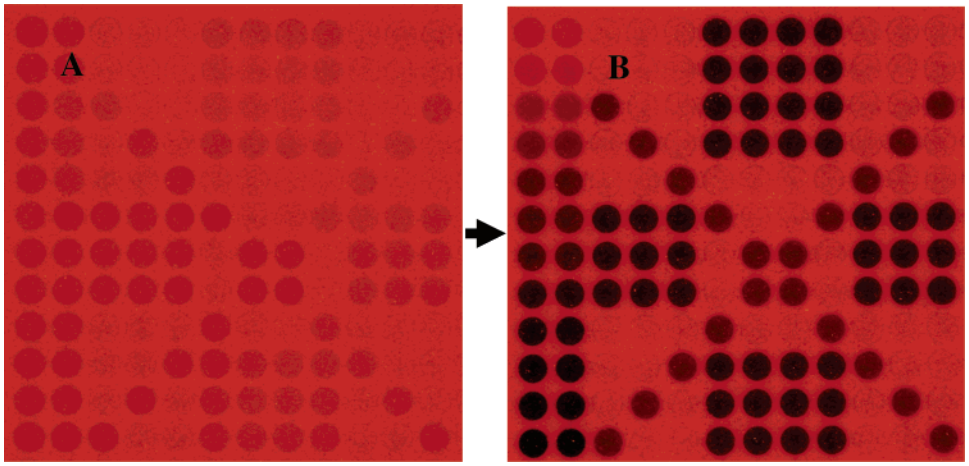

Figure 3. Pictures of the blank solvent (A) and sample library (B) plates using an optical filter with a passing-band at 600 ± 30 nm (transparency of 70% at 600 nm).

Table 1. Intensity of Light over the Corresponding Wells in Figure 3A

455672	**460202**	501583	505939	512201	**455543**	**446244**	**444504**	**449255**	503493	500450	496976
457471	**462152**	507880	512370	513310	**451500**	**445524**	**452860**	**448676**	508836	507810	503616
458982	**475901**	**472426**	514242	511492	**450573**	**452919**	**457983**	**450766**	504678	501759	**475437**
463952	**473618**	508847	**467748**	506448	**456584**	**455590**	**449349**	**448279**	505943	**477371**	509254
463605	**470384**	499472	502897	**468288**	505267	504680	504750	506163	**467415**	505114	512022
464893	**457176**	**451484**	**453824**	**455902**	**467047**	501643	504351	**466735**	**460527**	**454258**	**456597**
460547	**458843**	**461797**	**456645**	**465585**	501942	**470501**	**463253**	505703	**453503**	**457516**	**460453**
456690	**456944**	**461578**	**461921**	**461645**	503151	**460953**	**470138**	508547	**455748**	**464008**	**458526**
457342	**458275**	501097	498583	503103	**469650**	505491	504055	**465631**	506981	508200	510279
457455	**456061**	498798	499529	**469138**	**462724**	**453013**	**449918**	**457304**	**472773**	506283	504813
454272	**455198**	499331	**463838**	497858	**456237**	**456992**	**457167**	**452103**	505641	**467971**	505188
451376	**451148**	**463451**	498298	497948	**454231**	**451941**	**450573**	**457409**	500724	496907	**463273**

Table 2. Intensity of Light over the Corresponding Wells in Figure 3B

454167	**457629**	506167	503824	501415	**149660**	**142665**	**138243**	**141362**	491650	493829	495188
422091	**418674**	504450	504915	502333	**145943**	**142749**	**147467**	**141112**	499829	498486	490345
326841	**323504**	220860	503438	503229	**147144**	**143292**	**148600**	**146143**	499977	499770	**221614**
263884	**258972**	498910	**220658**	501041	**151307**	**145064**	**145101**	**144157**	498272	**224040**	499028
214495	**215430**	505262	500875	**220855**	501346	505234	502349	495197	**220380**	497507	499837
203044	**196729**	**149620**	**152104**	**147249**	**220758**	504096	**503011**	**220533**	**149794**	**152825**	**152185**
189693	**183421**	**152961**	**150901**	**154683**	500852	**220971**	**220476**	499692	**152084**	**154532**	**151726**
151002	**150752**	**154602**	**152914**	**151068**	502244	**220538**	**220631**	498795	**153310**	**153139**	**153654**
127696	**122237**	501887	506726	500121	**220263**	499678	498448	**226678**	499691	499087	496272
109863	**108748**	501227	505083	**220666**	**156713**	**149387**	**145432**	**148956**	220543	497173	500591
96191	**98762**	500604	**220703**	500586	**150741**	**147443**	**148303**	**143047**	499541	**220899**	490404
76407	**81212**	**220575**	505232	505205	**150914**	**150745**	**150173**	**150968**	500643	494097	**220480**

Table 3. Absorption Intensity of the Substrate Library

standard samples		testing samples									
1505	2574				305883	303579	306261	307893			
35380	43478				305557	302775	305393	307564			
132141	152397	251566			303429	309627	309383	304623			253823
200068	214646		247090		305277	310526	304248	304122		253331	
249110	254954			247433					247035		
261849	260447	301864	301720	308653	246289			246202	310733	301433	304412
270854	275422	308836	305744	310902		249530	242777		301419	302984	308727
305688	306192	306976	309007	310577		240415	249507		302438	310869	304872
329646	336038				249387			238953			
347592	347313			248472	306011	303626	304486	308348	252230		
358081	356436		243135		305496	309549	308864	309056		247072	
374969	369936	242876			303317	301196	300400	306441			242793

(transparency of 70% at 600 nm) was chosen for Cr^{3+} analysis. The standard samples (65 μL for each well, placed into the left 2 columns) and substrate solutions (65 μL for each well) were transferred onto the quartz sand-loaded sample plate, and then the sample plate was placed under the CCD camera to take a picture (Figure 3B). The two columns of samples on the left in the picture are the standard samples, and the others are testing samples. The intensity of the picture was converted to data format (Table 2).

From the data, we can calculate the absorption value, A_{ij} (i represents the row number in Tables 1 and 2 and j represents the column number in Tables 1 and 2), according to the data in Tables 1 and Table 2 with the formula

$$A_{ij} = B_{ij} - C_{ij}$$

where B_{ij} is the value in row i and column j in Table 1 and C_{ij} is the value in row i and column j in Table 2. The A_{ij} values are listed in Table 3.

From the data for the standard samples in Table 3, we obtained the calibration curve of Figure 4. In the calculation of the concentration, we use a value-comparing model. The software (IIDR) procedure for the calculation of the concentration is to take an absorption value A_{ij} from the test samples and compare it with the absorption values of the standard samples to determine the two absorption values,

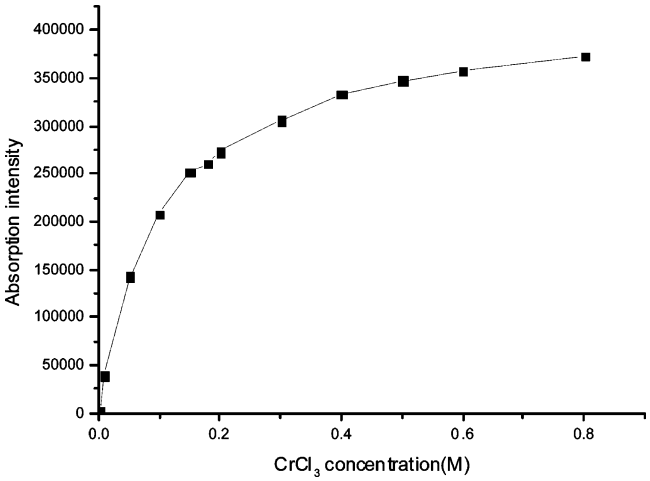

Figure 4. Calibration curve from the data of the left two columns in Table 3.

A_{x-1} and A_{x+1}, that are the closest to the absorption value A_{ij} where $A_{x-1} < A_{ij} < A_{x+1}$. We can find the corresponding concentrations M_{x-1} and M_{x+1} for A_{x-1} and A_{x+1}, respectively, on the calibration curve. Therefore, the concentrations of the testing samples can be calculated as

$$M_{ij} = M_{x-1} + (A_{ij} - A_{x-1})[(M_{x+1} - M_{x-1})/(A_{x+1} - A_{x-1})].$$

Table 4. Measured Molar Concentrations ($\times 10^{-1}$ M) of the $CrCl_3$ Samples in the Substrate Library

			3.00	2.93	3.01	3.07			
			2.99	2.90	2.98	3.06			
1.49			2.92	3.14	3.13	2.96			1.56
	1.44		2.98	3.17	2.95	2.94		1.54	
		1.45					1.44		
2.88	2.87	3.10	1.44			1.43	3.18	2.86	2.95
3.11	2.99	3.18		1.47	1.40		2.86	2.91	3.10
3.04	3.11	3.17		1.37	1.47		2.89	3.18	2.97
			1.47			1.47			
		1.46	3.00	2.93	2.96	3.09	1.51		
	1.40		2.99	3.13	3.11	3.12		1.44	
1.40			2.92	2.86	2.83	3.02			1.40

According to the method described above, we can calculate the concentrations of substrate samples. The results are listed in Table 4. (The concentration of the samples that we placed along the cross lines of the library is 0.15 M and the rest of the samples have a concentration of 0.30 M.) The relative errors are listed in Table 5. In the analysis, relative errors between −9.0 and 7.0% were achieved. The two $CrCl_3$ solutions (0.15 and 0.30 M) were also analyzed on a UV spectrometer. The concentrations of the two solutions from the UV spectrometer analysis are 0.145 M (relative error −3.4%) and 0.295 M (relative error −1.7%), respectively, which are consistent with that from CDRI analysis.

Table 5. Analysis Errors (%) of the Corresponding Concentrations in Table 4 Compared with the Prepared Concentrations

			−0.06	−2.40	0.40	2.42			
			−0.39	−3.22	−0.56	2.01			
−0.35			−2.55	4.57	4.27	−1.34			3.93
	−3.69		−0.67	5.68	−1.72	−1.85		2.85	
		−3.43					−3.73		
−4.14	−4.29	3.36	−4.29			−4.35	5.94	−4.58	−1.55
3.59	−0.20	6.15		−1.87	−6.91		−4.59	−3.00	3.45
1.28	3.80	5.75		−8.67	−1.88		−3.56	6.11	1.09
			−1.97			−2.30			
		−2.66	0.09	−2.35	−1.48	2.98	0.43		
	−6.64		−0.45	4.47	3.62	3.86		−3.70	
−6.83			−2.67	−4.82	−5.63	0.62			−6.89

3. Results and Discussion

In the control experiment, we performed colorimetric imaging analysis of samples in a transmission cell array. The cells have a top−bottom window configuration. The incidence light irradiates through the cells containing sample solutions from the bottom windows then comes out from the top of the solution samples to reach the camera detector. A picture of cells filled with water (each 100 μL) is shown in Figure 5A, and the relative errors are shown in Figure 5B (see Supporting Information B for calculation). The relative errors are from −16 to 11%. For a blank library, these

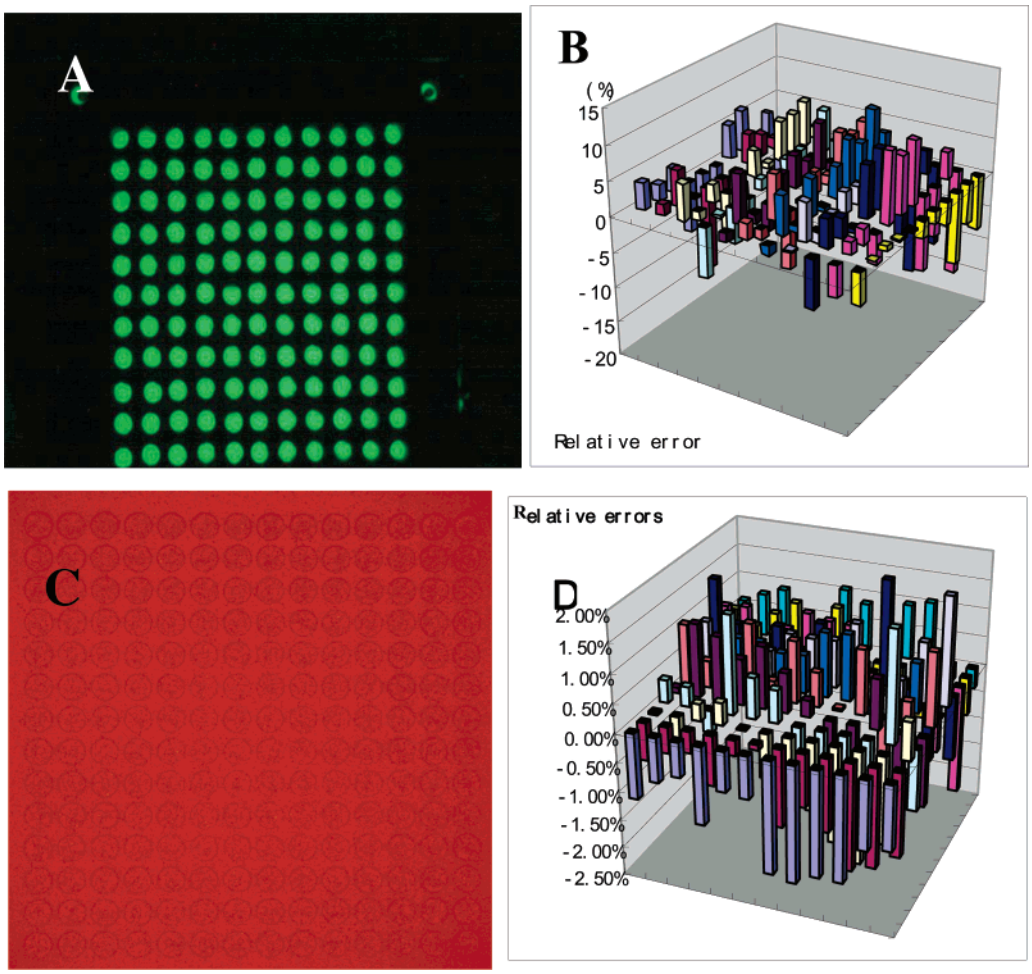

Figure 5. (A) Picture of the transmission cell array with water (each cell contains 100 μL), (B) the relative errors of the water samples in the transmission cells, (C) picture of the quartz sand-filled library plate using an optical filter with a passing-band at 600 ± 30 nm (transparency of 70% at 600 nm), and (D) the relative errors of quartz samples.

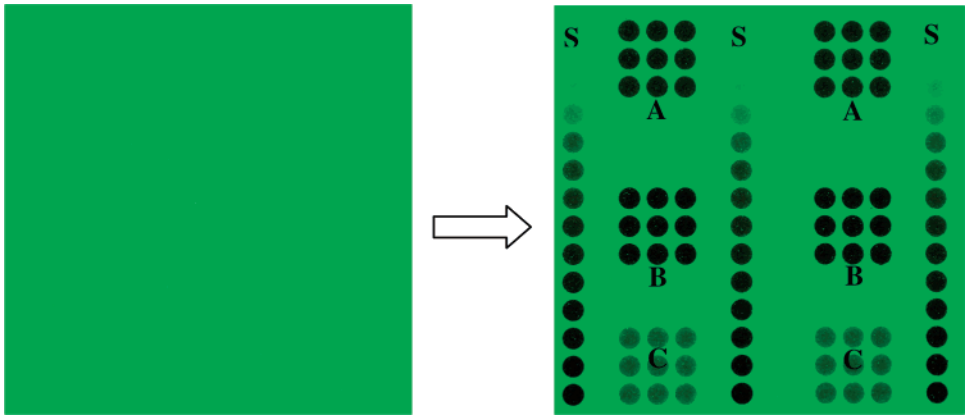

Figure 6. Pictures of the background and sample library using an optical filter with a passing-band at 540 ± 30 nm (transparency of 50% at 540 nm).

analysis errors are too big to be acceptable. The big errors come from the random light reflection and diffraction on the boated sample surfaces (the surface distorted to different shapes from sample to sample). When in the diffusion−reflection mode, the wells of the substrate plate (Figure 2) were filled with quartz sand, a picture of which is shown in Figure 5C, and the relative errors are shown in Figure 5D. The relative errors are from −2.0 to 2.0%. The results indicate that the diffusion−reflection method is more accurate than the transmission method. For purposes of comparison, the diffusion−reflection experiment has also been performed without the quartz sand, which gives −58 to 25% relative errors (Supporting Information B). This is because the top surfaces of the liquid samples are not flat; therefore, they reflect light randomly.

The results, shown in Figure 5D (see the numbers in Supporting Information B, Table 3s), show that most of the negative errors are found in the edge areas of the plate and most of the positive errors are located in the center of the plate. The results indicate that the light in the center of the plate is stronger than that in the edge areas. However, for most of the rapid analysis, an error within −2.0 to 2.0% is tolerable.

From the example in the Cr^{3+} ion analysis, the results indicate that the analysis method is based on the diffusion−reflection of the light in samples. Before the light reaches the detector, it has been reflected many times on quartz surfaces and absorbed many times by the solution that fills the gaps among the quartz particles. The absorption does not follow Bill's law. Therefore, the absorption intensity−concentration curve is not a straight line. However, a relatively good linearity can be obtained in the low-concentration side on the calibration curve. If we draw a tangent of the calibration curve through (0, 0), we can calculate the slope of the tangent (using a in-house-designed program). In the calculation of the slope, the concentration of solution is moles per liter. We define it as Sl (units of abs/M). The Sl parameter is related to the characteristic absorption capability of specific compound, the band-passing property of the optical filter employed, the spectral response of CCD camera, the particle size of quartz sand, and the intensity of light source. In our investigation, the CCD camera, the particle size of quartz sand, and the light source are fixed. The Sl value will mainly depend on the characteristic absorption capability of the specific compound and the band passing property of the optical filter. For the Cr^{3+} analysis, when an optical filter with a passing band at 600 ± 30 nm (transparency of 70% at 600 nm) is chosen, the Sl is 3.94×10^6 abs/M. It is clear that a high-Sl value corresponds to an high-analysis sensitivity.

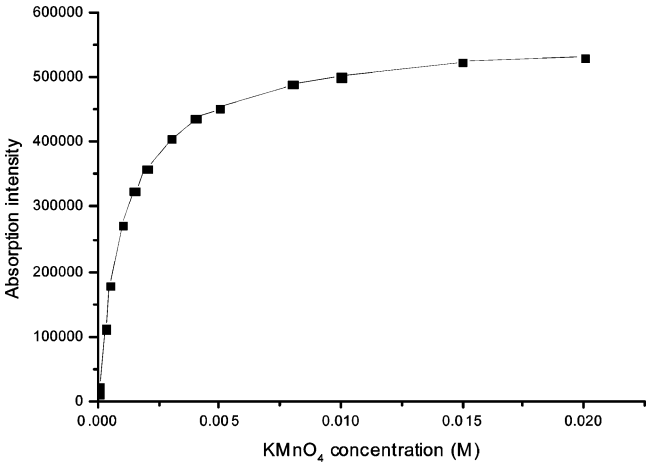

Figure 7. Calibration curve of the $KMnO_4$ solutions.

3.1. Analysis of $KMnO_4$ Solutions. The $KMnO_4$ solutions were analyzed, using the same method, to evaluate our method and instrument. In this study, $KMnO_4$ standard solutions with concentrations of 0.020, 0.015, 0.010, 0.0080, 0.0050, 0.0040, 0.0030, 0.0020, 0.0015, 0.0010, 0.00050, and 0.00030 M, respectively, were prepared. The solutions with concentrations of 0.0040, 0.010, and 0.0010 M were also employed as testing solutions. The samples are placed as shown in Figure 6. The three columns labeled with "S" are standard samples (in an increasing concentration order from top to bottom). The samples labeled with "A" have concentration of 0.0040 M; those labeled with "B" have concentration of 0.010 M, and those labeled with "C" have concentration of 0.0010 M. In the analysis, an optical filter with passing-band at 540 ± 30 nm (transparency of 50% at 540 nm) was chosen. The characteristic absorption band of permanganate potassium is centered at 542 nm.

From the digital picture in Figure 6 a calibration curve was obtained (Figure 7) after the calculation process (automatically performed by the computer). After the same calculation process described in the Experimental Section

Table 6. Measured Concentrations (M) of the $KMnO_4$ Test Samples

3.93×10^{-3}	3.95×10^{-3}	4.25×10^{-3}	3.93×10^{-3}	4.12×10^{-3}	3.73×10^{-3}
4.05×10^{-3}	3.75×10^{-3}	3.98×10^{-3}	3.76×10^{-3}	3.99×10^{-3}	3.89×10^{-3}
3.74×10^{-3}	4.28×10^{-3}	3.96×10^{-3}	3.84×10^{-3}	4.06×10^{-3}	3.82×10^{-3}
1.05×10^{-2}	9.86×10^{-3}	9.72×10^{-3}	9.54×10^{-3}	9.78×10^{-3}	9.30×10^{-3}
1.08×10^{-2}	9.87×10^{-3}	1.00×10^{-2}	1.03×10^{-2}	1.05×10^{-2}	9.08×10^{-3}
1.07×10^{-2}	9.86×10^{-3}	9.90×10^{-3}	1.01×10^{-2}	1.09×10^{-2}	$9.44 \times 10^{-3}3$
1.05×10^{-3}	1.01×10^{-3}	9.58×10^{-4}	9.26×10^{-4}	9.20×10^{-4}	9.47×10^{-4}
1.04×10^{-3}	1.04×10^{-3}	9.57×10^{-4}	9.78×10^{-4}	1.01×10^{-3}	9.80×10^{-4}
9.71×10^{-4}	1.04×10^{-3}	9.39×10^{-4}	9.80×10^{-4}	1.01×10^{-3}	9.54×10^{-4}

Table 7. Corresponding Analysis Errors (%) from the Comparison of the Measured Concentrations with the Prepared Concentrations[a]

−1.85	−1.37	6.32	−1.84	3.11	−6.81
1.30	−6.17	−0.53	−6.07	−0.21	−2.83
−6.49	7.06	−1.03	−3.97	1.53	−4.50
5.45	−1.36	−2.78	−4.60	−2.16	−7.00
8.03	−1.27	0.46	2.84	5.37	−9.18
6.66	−1.41	−1.00	0.60	9.20	−5.63
5.28	1.29	−4.25	−7.36	−8.02	−5.32
4.44	4.23	−4.30	−2.18	−0.67	−2.03
−2.93	4.49	−6.11	−2.01	0.93	−4.57

[a] 0.0040 M (the top 3 rows), 0.010 M (the middle three rows), and 0.0010 M (the bottom three rows).

was conducted, the concentrations of the test solutions are listed in Table 6, and the corresponding errors are listed in Table 7. The relative errors are below 10.0%. The Sl value calculated from the calibration curve is 3.73×10^8 abs/M. The Sl value (3.73×10^8) of MnO_4^- is bigger than that of Cr^{3+} (3.94×10^6). It means that the analysis method is more sensitive to MnO_4^- than Cr^{3+}. As mentioned before, the analysis error over the blank testing plate is in the region of −2.0 to 2.0%. The analysis errors are within 10.0% in the $KMnO_4$ analysis. The majority of our analysis error might come from the three sources: the hand transferring of liquid samples by micropipettor, the accuracy of the standard solutions, and the calculation model of the concentration. We have evaluated the relative errors in the solution transfer by measuring 65 μL samples of water and weighing them on a balance (10 samples). The relative errors are from −1.3 to 1.2%. We think that the analysis errors from this source can be further reduced by employing a robot to transfer the liquid samples. If we prepare the solution carefully, we can achieve high accuracy in the standard solutions. The other source of analysis error comes from the calculation mode of the concentrations. In the concentration calculation, we use a value-comparing mode. For this calculation mode, to reach a high accuracy, we need as many standard solutions as possible to build up a calibration curve. This is a time- and labor-consuming job. Therefore, a better way may be the modification of the calculation software, as discussed later.

3.2. Analysis of Methylene Blue Solutions. To test our methodology in organic compound analysis, we conducted an experiment on methylene blue analysis. Standard solutions with concentrations of 0.0010, 0.00075, 0.00050, 0.00030, 0.00020, 0.00010, 0.000075, 0.000050, 0.000030, 0.000020, 0.0000075, and 0.0000050 M were prepared. The standard samples are placed in the left two columns (labeled "S") as shown in Figure 8. Solutions with methylene blue concentrations of 0.000050 and 0.00020 M were employed as the test solutions. Solution samples with a methylene blue concentration of 0.00020 M were placed along the two cross-lines, and samples with a methylene blue concentration of 0.000050 M were placed in those squares as shown in the picture of Figure 8. The characteristic absorption band of methylene blue is centered at 464 nm. Therefore, an optical filter with passing-band at 460 ± 30 nm (transparency of 70% at 460 nm) was chosen.

After the same calculations described in the Experimental Section were performed, the calibration curve, the measured concentration numbers of methylene blue solutions, and the relative analysis errors were obtained, as shown in Figure 9 and Tables 8 and 9, respectively. The testing solutions were also analyzed with a regular UV spectrometer. The concentrations of the two solutions measured by the UV spectrometer are 1.97×10^{-4} and 4.63×10^{-5} M, respectively. The results analyzed by CDRI (Table 8) are consistent with those analyzed by the UV spectrometer within a relative error of

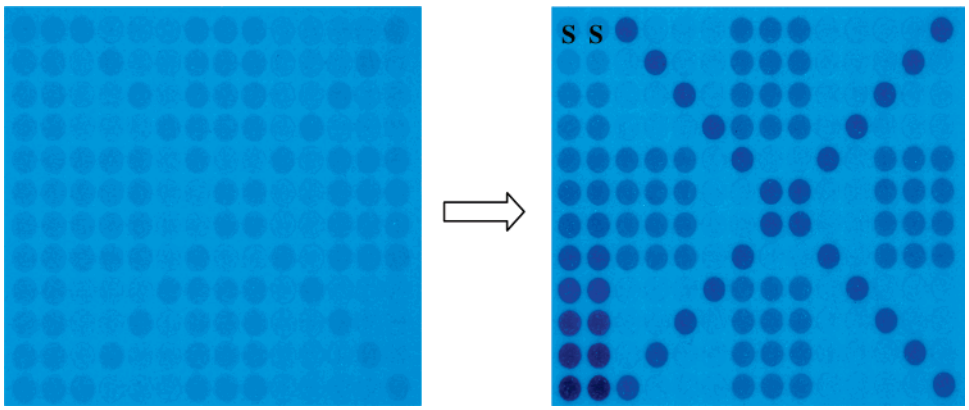

Figure 8. Digital picture of the background and sample library with an optical filter with a passing-band at 460 ± 30 nm (transparency of 70% at 460 nm).

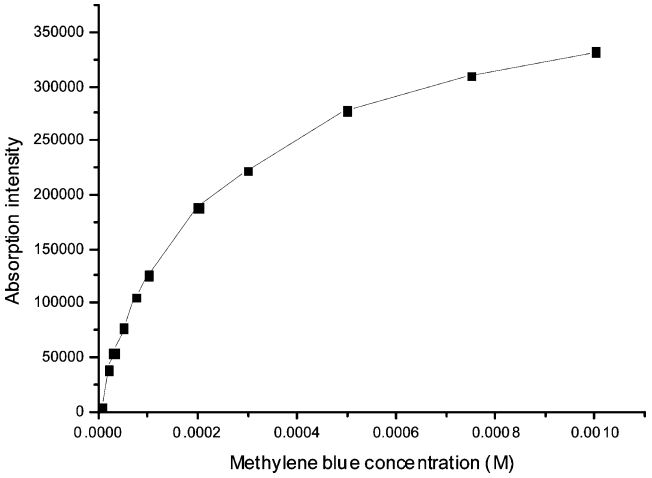

Figure 9. Calibration curve of methylene blue.

8.0%. The Sl value from the calibration curve is 1.93×10^9 abs/M, which is bigger than that (3.73×10^8) of $KMnO_4$. It can be seen that this is a very sensitive method for methylene blue analysis. The analysis errors in Table 9 are within −8.0 to 2.6%. The analysis errors are at the same level as those in the $CrCl_3$ and $KMnO_4$ analyses.

As an application of the colorimetric high-throughput analysis method, we conducted acrolein analysis. In the analysis, fuchsin sulfate was employed as indicator. The light yellow fuchsin sulfate solution can react with acrolein to form a purple solution that has strong absorption at 589 nm (see Supporting Information C for UV spectra of the compounds). An optical filter with passing-band at 600 ± 30 nm was selected for the analysis. The fuchsin sulfate solution (2.00 mL, 0.00020 M) was transferred into sample plate with a well array (14 × 14 wells, well diameter 1.0 cm, volume 4.0 mL). In the experiment, standard acrolein water solutions with concentrations of 0.80, 0.70, 0.60, 0.50, 0.40, 0.30, 0.20, 0.10, 0.080, 0.060, 0.040, 0.020, and 0.010 M were prepared.

Before applying the technology to the practical analysis of acrolein, we performed a control experiment. We placed 8 samples with acrolein concentrations of 0.40 M in the first row, 0.30 M in the second row, and 0.20 M in the third row on the testing plate. The standard solutions of acrolein were also placed into the plate. After analysis by the CDRI method, the calibration curve in Figure 10 was obtained. The concentrations are listed in Table 10. The concentration for entry 1 is very close to 0.40 M; the concentration for entry 2 is very close to 0.30 M, and that for entry 3 is very close to 0.20 M. The relative errors (the concentrations obtained from CDRI compared with the prepared concentrations 0.40, 0.30, and 0.20 M) are listed in Table 11. Relative errors within −6.0 to 7.0% were reached. The errors are within the same region as that in the previous analysis. We think that this error region is permissable in our primary screening of catalysts. The Sl is 3.91×10^6 abs/M for acrolein analysis.

In the practical application for acrolein analysis, we collected 64 acrolein samples in a well-array (14 × 14 wells, well volume 4.0 mL, each well contains 2.00 mL of fuchsin sulfate solution (0.00020 M)) sample plate from a 64-channel fixed-bed reactor (will be published separately) that runs the propylene oxidation reaction. The standard acrolein solutions

Table 8. Measured Methylene Blue Concentrations (M)

2.05×10^{-4}				5.00×10^{-5}	5.02×10^{-5}	5.00×10^{-5}						1.92×10^{-4}
	1.94×10^{-4}			5.07×10^{-5}	5.07×10^{-5}	5.01×10^{-5}					1.90×10^{-4}	
		1.90×10^{-4}		5.05×10^{-5}	5.05×10^{-5}	5.01×10^{-5}				1.95×10^{-4}		
			1.94×10^{-4}	5.01×10^{-5}	5.06×10^{-5}	5.01×10^{-5}			1.91×10^{-4}			
4.95×10^{-5}	5.04×10^{-5}	5.03×10^{-5}		1.92×10^{-4}				1.97×10^{-4}		4.93×10^{-5}	5.05×10^{-5}	5.08×10^{-5}
5.00×10^{-5}	4.99×10^{-5}	5.02×10^{-5}			1.96×10^{-4}	2.03×10^{-4}				4.96×10^{-5}	5.02×10^{-5}	5.03×10^{-5}
5.04×10^{-5}	5.03×10^{-5}	5.05×10^{-5}			1.98×10^{-4}	1.89×10^{-4}				4.92×10^{-5}	4.95×10^{-5}	5.04×10^{-5}
5.07×10^{-5}	5.04×10^{-5}	5.02×10^{-5}		2.00×10^{-4}			1.96×10^{-4}			5.05×10^{-5}	4.91×10^{-5}	4.89×10^{-5}
			1.89×10^{-4}	5.04×10^{-5}	4.64×10^{-5}			1.87×10^{-4}				
		1.88×10^{-4}		4.83×10^{-5}	5.04×10^{-5}	4.80×10^{-5}				1.94×10^{-4}		
	2.00×10^{-4}			4.65×10^{-5}	4.76×10^{-5}	4.81×10^{-5}					2.00×10^{-4}	
1.92×10^{-4}				4.70×10^{-5}	4.80×10^{-5}	4.82×10^{-5}						1.88×10^{-4}

Table 9. Corresponding Analysis Errors (%) of the Methylene Blue Samples by Comparison with the Prepared Methylene Blue Samples[a]

2.55					0.00	0.40	0.00			−4.10
	−3.00				1.40	1.40	0.20		−4.95	
		−3.76			1.00	1.00	0.20	−2.40		
			−3.25		0.20	1.20	0.80	−4.75		
−1.00	0.80	0.60		−2.34			−1.75	−1.40	1.00	1.60
0.00	−0.20	0.40			−1.90	1.30		−0.80	0.40	0.60
0.80	0.60	1.00			−1.10	−5.30		−1.60	−1.00	0.80
1.40	0.80	0.40		1.73			−1.90	1.00	−1.80	−2.20
			−5.55		0.80	0.80	−7.20	−6.40		
		−6.05			−3.40	0.80	−4.00	−2.80		
	−0.20				−7.00	−4.80	−3.80		−0.15	
−3.80					−6.00	−4.00	−3.60			−6.15

[a] Concentrations of 0.00020 M (on the cross lines and center square) and 0.000050 M (the rest of the squares).

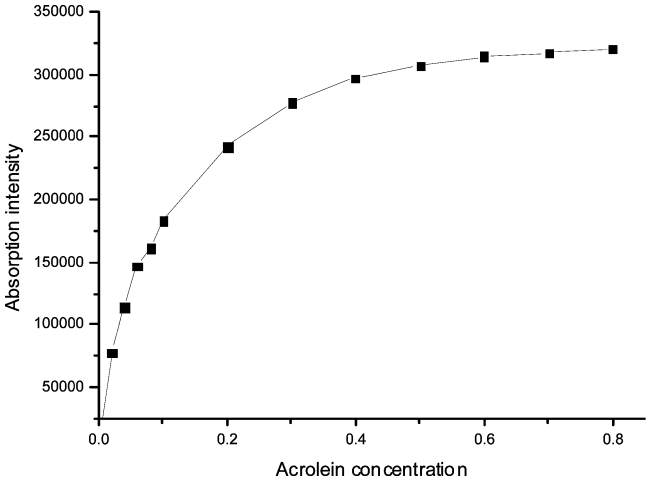

Figure 10. Calibration curve of acrolein.

Table 10. Concentrations Measured by CDRI Method

entry	concentrations ($\times 10^{-1}$ M)							
1	3.87	4.17	4.00	3.84	4.03	3.96	3.96	4.21
2	2.97	3.03	3.17	2.95	3.05	2.97	2.83	2.97
3	1.99	2.13	1.97	1.99	1.90	2.00	1.98	1.91

Table 11. Relative Errors for CDRI Method

entry	errors (%)							
1	−3.2	4.2	0	−4.0	0.75	−1.0	−1.0	5.2
2	−1.0	1.0	5.6	−1.7	1.7	−1.0	−5.7	−1.0
3	−0.5	6.5	−1.5	−0.5	5.0	0	−1.0	−4.5

were also transferred into the wells of the sample plate. After the samples were kept at room temperature for 30 min, 65 μL aliquots of the samples were transferred into the corresponding wells of the testing plate for analysis. After going through the analysis process described in the Experimental Section, the concentrations of acrolein solutions (Table 12) were obtained. To confirm the reliability of our analysis method, we also checked the three solutions labeled A, B, and C in the upper left corner of Table 12, entry 1, by GC (with thermal conductivity detector). The concentrations analyzed from GC are 0.487, 0.339, and 0.169 M, respectively. In Table 12, the concentrations of the solutions from our CDRI analysis are 0.467, 0.325, and 0.161 M, respectively. The relative errors of the CDRI method, compared to the GC method (the results of GC analysis taken as standard), are −4.1, −4.1, and −4.7%, respectively. We think that both of the analysis methods gave very close results, within the error region of 0−5.0%. The method developed for acrolein analysis is potentially useful in the analysis of acrolein from a high-throughput parallel fixed-bed reactor. From this example, by making use of chemical reactions, we can also analyze compounds that do not have characteristic absorption bands in the visible light spectrum by the colorimetric imaging technology.

In the current investigation, our CDRI technology gives total relative analysis errors below 10.0%. The light intensity difference over the testing plate leads to analysis errors of about 2.0%. The other sources leading to analysis error are from the manual transfer of the solutions, the accuracy of the standard solution concentration, and the calculation mode of the calibration curve. If a robot were employed to transfer solutions, the analysis error could be reduced to an even lower level. Another source of the analysis error comes from the calculation mode of the calibration curve. With the current calculation mode, to improve the analysis accuracy, we need as many standard solutions as possible; this will require a lot of labor and time to prepare standard solutions with accurate concentrations. On the other hand, we can change the calculation method to a different mathematics mode. In the current calculation, the calibration curve is drawn on the basis of straight lines between two nearby data points. It is predicted that the accuracy can be improved by changing the straight lines between data points to cirque or parabola curves. For this, we need to design new data reduction program. This work is still in progressing.

Table 12. Measured Concentration Values of the Acrolein Samples from a Parallel Fixed-Bed Reactor

entries	acrolein concentrations (M)							
1	**0.467 (A)**	**0.325 (B)**	**0.161 (C)**	9.60×10^{-2}	8.38×10^{-2}	6.77×10^{-2}	1.01×10^{-1}	2.00×10^{-2}
2	2.00×10^{-2}	7.46×10^{-2}	8.24×10^{-2}	7.15×10^{-2}	8.90×10^{-2}	2.09×10^{-2}	1.00×10^{-1}	2.00×10^{-2}
3	7.77×10^{-2}	7.87×10^{-2}	2.00×10^{-2}	4.78×10^{-2}	7.17×10^{-2}	7.10×10^{-2}	9.39×10^{-2}	9.75×10^{-2}
4	3.74×10^{-2}	6.50×10^{-2}	2.00×10^{-2}	4.88×10^{-2}	7.40×10^{-2}	7.55×10^{-2}	8.21×10^{-2}	2.00×10^{-2}
5	2.00×10^{-2}	6.87×10^{-2}	8.36×10^{-2}	3.62×10^{-2}	8.53×10^{-2}	2.55×10^{-2}	9.70×10^{-2}	1.10×10^{-1}
6	2.00×10^{-2}	4.83×10^{-2}	8.03×10^{-2}	3.54×10^{-2}	2.24×10^{-2}	7.74×10^{-2}	1.01×10^{-1}	1.00×10^{-1}
7	2.00×10^{-2}	5.33×10^{-2}	2.77×10^{-2}	2.44×10^{-2}	6.24×10^{-2}	2.94×10^{-2}	9.28×10^{-2}	2.45×10^{-2}
8	2.00×10^{-2}	3.93×10^{-2}	7.18×10^{-2}	2.00×10^{-2}	6.63×10^{-2}	6.60×10^{-2}	2.41×10^{-2}	2.00×10^{-2}

Comparing the CDRI analysis method with the UV spectrometer, we confirmed that our CDRI technology gave reasonable results (as in the analysis of the $CrCl_3$ and methylene blue solutions). In the analysis of acrolein, the results from our CDRI methodology are consistent with that from the traditional gas chromatography analysis.

Although, we developed a photofluorescence imaging technology for library analysis in our previous research work,[4] the photofluorescence imaging technology is only valid for the fluorescent compounds. The novelty of the current work is that it could be applied in analysis of compounds that have characteristic absorption bands in visible light. The basis of the CDRI technology is the measurement of the intensity of the diffusion−reflection light from the samples, which is different from the measurement of the fluorescent light intensity in photofluorescence imaging technology. Although the commercially available high-throughput UV−vis spectroscopy and plate readers mentioned in the Introduction (i.e., the one from Molecular Devices Corp.) could do high-throughput analysis, most of them use a serial screening mode. They are actually automated regular UV−vis spectrometers with a cell array driven by a step motor. In this mode, the machine screens samples one by one. The throughput is not as high as the current CDRI imaging technology. The other issue is that because the commercial instrument includes a lot of moving parts and an UV−vis spectrometer, it is much more expensive than our CDRI machine (see Supporting Information D for the cost of the CDRI machine). The other drawback of the high-throughput UV−vis spectrometers is that one needs to know the concentration region of the samples already; otherwise, it is very easy to be saturated (for regular UV−vis spectroscopy also). In our approach, the concentration region is much wider, usually 10 times. Because the light is reflected back to the camera from different depths of the samples, the solution and the quartz sands do not absorb all of the light. Therefore, it is not necessary to know in detail about the concentration region of the solutions. As proven by us previously, the diffusion−reflection mode is more accurate than the transmission mode for the CDRI analysis method. The big analysis errors in the transmission mode come from the random reflection and diffraction of light on the boated-up surface of the samples. Although, we have not seen literature addressing this problem for the commercial high-throughput UV−vis spectroscopy and plate readers, it still exists in these analysis approaches. In diffusion−reflection mode, the current CDRI technology effectively avoids the problem.

Comparing our CDRI technology with the reported high-throughput analysis technologies, such as IR thermography,[1−3] laser-induced resonance-enhanced multiphoton ionization,[5] HPLC screening technology,[6] microprobe-sampling mass spectrometry,[7−8] fluorescence indicators,[9−10] and UV−vis spectroscopy plate readers, we think that the CDRI technology offers a new option for high-throughput analysis, and we also think that it could find much wider applications in chemical analysis.

Conclusion

The current research work shows the development of a high-throughput technology based on colorimetric diffusion−reflection imaging. This technology is valid for analysis of organic and inorganic compounds with characteristic absorption bands in visible light. The application of quartz sands as light reflection media makes it possible to employ the CDRI technology to analyze liquid samples and guarantee low-relative analysis errors. We believe that, if a UV-sensitive CCD camera is employed as detector, this technology could also be extended to the ultraviolet light region which would make it even more widely applicable in high-throughput analysis.

Acknowledgment. This project was supported by NSFC (20327003).

Supporting Information Available. Diagram of a commercial serial-mode UV−vis spectrometer, discussions of the transmission-mode cell array and diffusion−reflection error calculations and of the cost of the analysis, tables showing the relative errors, and figures showing a methylene blue library, the molecular structure of fuchsin sulfate, the UV spectra of fuchsin sulfate and fuchsin sulfate/acrolein. This material is available free of charge via the Internet at http://pubs.acs.org.

References and Notes

(1) Moates, F. C.; Somani, M.; Annamalai, J.; Richardson, J. T.; Luss, D.; Wilson, R. C. *Ind. Eng. Chem. Res.* **1996**, *35*, 4801.
(2) Taylor, S. J.; Morken, J. P. *Science* **1998**, *280*, 267.
(3) Wilson, R. C. International Patent WO9732208, 1997.
(4) Dai, Q. X.; Xiao, H. Y.; Li, W. S.; Na, Y. Q.; Zhou, X. P. *J. Comb. Chem.* **2005**, *7*, 539.
(5) Senkan, S. M. *Nature* **1998**, *394*, 350.
(6) Jaramillo, T. F.; Ivanovskaya, A.; McFarland, E. W. *J. Comb. Chem.* **2002**, *4*, 17.
(7) Cong, P.; Doolen, R. D.; Fan, Q.; Giaquinta, D. M.; Guan, S.; McFarland, E. W.; Poojary, D. M.; Self, K.; Turner, H. W.; Weinberg, W. H. *Angew. Chem., Int. Ed.* **1999**, *38*, 484.
(8) Cong, P.; Dehestani, A.; Giaquinta, D.; Guan, S.; Markov, D.; Self, K.; Turner, H.; Weinberg, H. *Proc. Natl. Acad. Sci. U.S.A.* **1999**, *96*, 11077.
(9) Reddington, E.; Sapienza, A.; Gurau, B.; Viswanathan, R.; Sarangapani, S.; Smotkin, E. S.; Mallouk, T. E. *Science* **1998**, *280*, 1735.
(10) Miller, S. J.; Copeland, G. T. *J. Am. Chem. Soc.* **1999**, *121*, 4306.
(11) Nakayama, A.; Suzuki, E.; Ohmori, T. *Appl. Surf. Sci.* **2002**, *189*, 260.
(12) Busch, O. M.; Hoffmann, C.; Johann, T. R. F.; Schmidt, H. W.; Strehlau, W.; Schuth, F. *J. Am. Chem. Soc.* **2002**, *124*, 13527.

CC0600730